# A KINEMATIC STUDY AND 3D STRUCTURE OF THE OWL NEBULA*

Ma. T. García-Díaz[1], F., W. Steffen[1], W. J. Henney[2], F. García-López[3], J. A. López[1], D. González-Buitrago[4], A. Aviles[5]

tere@astro.unam.mx, wsteffen@astro.unam.mx, whenney@gmail.com, karia@gmail.com, jal@astro.unam.mx, gdiegohe@uci.edu, andres.aviles.alvarado@gmail.com

## ABSTRACT

*Subject headings:* ISM: planetary nebulae: general − planetary nebulae: individual (NGC 3587) − ISM: kinematics and dynamics − techniques: imaging spectroscopy

## 1. INTRODUCTION

NGC 3587, cataloged as M 97 and better known as the Owl Nebula because it presents two regions poor of material that resemble the eyes of an owl. While there are many planetary nebula that have a bipolar or multipolar structure of their main edge-brightened shells, NGC 3597 has a nearly spherical overall structure with a bipolar internal cavity. Only a few such objects are known (e.g. Abell 33, Abell 50 and, possibly, NGC 2242).

The Owl Nebula was one of the first nebulae observed by Messier (1764). It has been studied using deep imaging and low resolution spectroscopy with good coverage of the different emitting regions. The nebula has also been studied using high-resolution spectroscopy of specific areas of the nebula (Guerrero et al. 2003).

According to Chu, Jacoby, & Arendt (1987) and Kwitter, Chu, & Downes (1992), the Owl nebula consists of three shells, a double shell surrounding the main nebula and an outer halo with an arc shape. The authors find that the halo is interacting with the surrounding interstellar medium.

The first kinematic study of the nebula was done by Sabbadin et al. (1985), who performed a long slit high resolution spectroscopic study using an echelle spectrograph coupled to the 182 cm telescope at the Asiago Astronomical Observatory in Italy. Their observations were obtained at four slit positions with different position angles in the emission lines of H$\alpha$, [N II] and [O III]. Their study was focused only on the bright inner shell of the nebula. The authors conclude that the main part of NGC 3587 is a nonhomogeneous shell, with a nebular mass of 0.15 $M_\odot$ and a central star of mass 0.70 $M_\odot$.

Guerrero et al. (2003) presented an observational study of the nebula based on deep images in different filters and long slit echelle spectroscopy at two positions of the nebula in the emission lines of H$\alpha$, [O III] 5007 Å and [N II] 6584 with the main goal to build a spatio-kinetic model of the nebula including the structure and nature of the halo (Chu, Jacoby & Arendt 1987). For this model, the authors assumed that the material is moving homologously, but with each component of the model expelled at different times. They include essentially four structural and kinematic

*Based upon observations carried out at the Observatorio Astronómico Nacional on the Sierra San Pedro Mártir (OAN-SPM), Baja California, Mexico, which is operated by the Universidad Nacional Autónoma de México.

[1]Instituto de Astronomía, Universidad Nacional Autónoma de México. Km 103 Carretera Tijuana-Ensenada, 22860 Ensenada, Baja California, México

[2]Instituto de Radioastronomía y Astrofísica, Universidad Nacional Autónoma de México, Apartado Postal 3-72, 58090 Morelia, Michoacán, México

[3]Centro de Nanociencias y Nanotecnología, UNAM

[4]University of California - Irvine

[5]Facultad de Ingeniería Mecánica y Eléctrica de la Universidad Autónoma de Nuevo León

components: the outer halo, two nearly spherical shells, and a cavity in the inner shell with a bipolar, dumbbell shaped morphology. The authors found that the halo, with a diameter > 200 arcsec and low surface brightness, is asymmetrical with indications of interaction with the interstellar environment. Corradi et al. (2003) suggest that this is a recombination halo.

The white dwarf central star of NGC 3587 has a visual magnitude of 16.04 (Acker et al 1982) and was classified as hgO(H) by Napiwotzki & Schönberner (1995), which means high surface gravity and hydrogen-rich. The authors used low resolution spectroscopy, showing absorption lines in H$\beta$, H$\gamma$, H$\delta$, and He II. Górny et al. (1997), with evolutionary models to estimate a central star is of 0.854 $M_\odot$ while Napiwotzki (1999) found that the effective temperature of the central star to be 93,900± 5,600 $K$ and with a mass of 0.55 $M_\odot$.

Regarding the distance to the nebula, there are several methods to calculate the distances to PNs and for NGC 3587 this resulted in figures between 0.4 and 1.4 kpc (Guerrero et al., 2003, and references therein). One of the most recent methods used to calculate the distance to the Owl Nebula is that applied by Frew et al. (2016), who used the relative surface brightness of H$\alpha$ together with the radius of the nebula to calculate the distances of a considerable sample of PNs. Using that method the authors found a distance of 0.87 ± 0.26 kpc to the Owl Nebula, which is roughly in the middle of the earlier range of distance determinations. We adopt this value in our paper.

In this work we present an exhaustive spectroscopic study of the Owl Nebula with the aim to understand the remarkable bipolar structure of low level of emission in the Owl's eyes and its dynamic evolution. Using long slit spectroscopy data from OAN-SPM with full coverage of the bright shells we are able to construct a continuous cube of iso-velocity maps that help in their interpretation. Using the code *Shape* a morphokinematical model that reproduces the new data in more detail than previous models (Guerrero et al., 2003) we arrive at a new and more complex model of the inner cavities than a simple bipolar expansion of the fast wind from the central star.

We divide the paper as follows. In §2 we present the observations and results, in §3 we discuss the isovelocity channel maps, §4 describes the morphokinematic modeling with *Shape* and some physical interpretations are presented in §5.

## 2. OBSERVATIONS AND RESULTS

The observations of the planetary nebula NGC 3587 were obtained at the *Observatorio Astronómico Nacional* at *San Pedro Mártir*, (OAN-SPM), Baja California, Mexico, and were reduced by standard procedures in IRAF[1] to correct bias, extract cosmic, apply flat fields to remove the pixel-to-pixel response and calibrate the wavelength for the medium and high resolution spectra. The medium resolution spectroscopic data and direct images were flux calibrated.

### *2.0.1. Medium Resolution Observations*

Medium resolution spectroscopy was performed on 2015 June 23. We employed the Boller & Chivens (B&Ch) spectrograph attached to 2.1 m telescope. The spectra span the wavelength range from 3765 Å to 7260 Å. We used a 400 lines $mm^{-1}$ grating covering the wavelength range from 4560 Å to 5750 Å. A Marconi 13.5 $\mu$m $pix^{-1}$ CCD detector, with 2048 × 2048 pixels and no binning was used. Two observations with an east-west slit orientation were taken, one across the central star and another separated from it. The exposure time was 600 s per spectrum. The sky lines have been removed. A He-Ne-Ar comparison lamp was obtained after each spectrum to ensure good wavelength calibration. For flux calibration a standard star was observed at the end of the night, taken from the list of Landolt (1992) and Bohlin et al. (2001).

Figure (1) shows the stellar (left) and nebular spectra (right) of NGC 3587. The spectra for the nebula were extracted from the full length of the slit that covers the nebula.

The spectra of the nebula show Ne III, He I, He II, Balmer lines, O III, [N II], S II and Ar III emission lines.

[1]IRAF is distributed by the National Optical Astronomy Observatories, which is operated by the Association of Universities for Research in Astronomy, Inc. under cooperative agreement with the National Science foundation

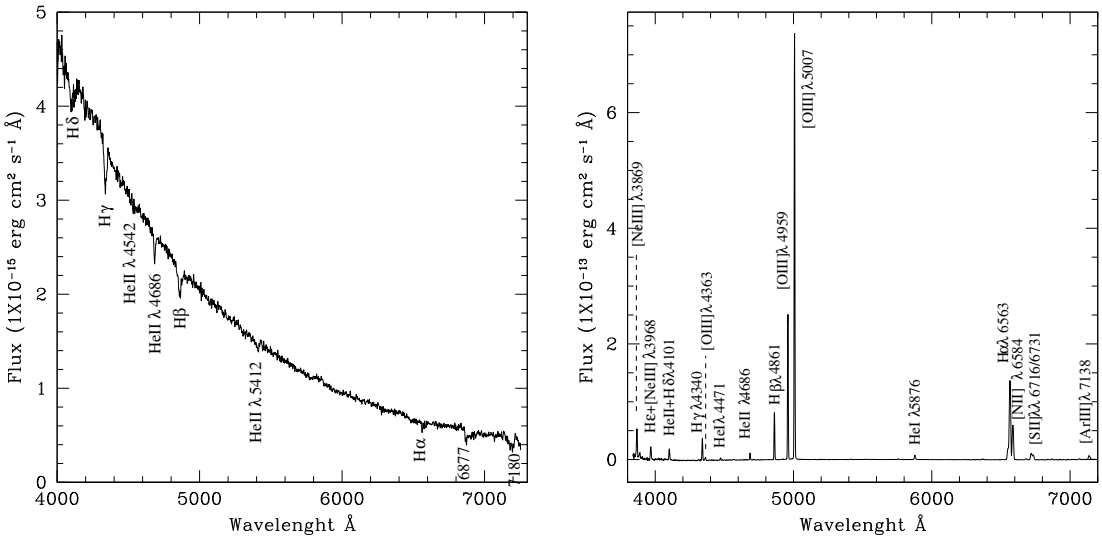


Fig. 1.— (a) Spectra of the central star of NGC 3587 (b) Nebular spectrum.

### *2.0.2. Optical Imaging*

A set of narrow-band CCD direct images of NGC 3587 were obtained on 2015 June 22 using the 0.84 m Telescope. The detector was a 2048 $X$ 2048 Marconi CCD (13.5 $\mu$m pixel size). The filters used to acquire the images were H$\alpha$ (bandwidth, $\Delta\lambda$ = 10Å, central wavelength, $\lambda_c$ = 6563Å), [O III]($\Delta\lambda$ = 50Å, $\lambda_c$ = 5007Å, $\Delta\lambda$ = 50Å) and [N II]($\Delta\lambda$ = 10Å, $\lambda_c$ XXXXÅ). Exposure times were 1800 s for each filter. The images were aligned with respect to each other. The flux was calibrated was using the standard star observed with B&Ch during the night of June 23rd, 2015.

Figure 2 is a mosaic of images of NGC 3587, the panels correspond to H$\alpha$(left), [N II] 6584 (center), and [O III] 5007 Å(right). Images are displayed at two different digital contrast levels to show the structure of the nebula and the big and weak halo. At the bottom, a color composite of the nebula is shown, where red is H$\alpha$, which is concentrated in the inner part of the nebula. [N II] 6584 emission, shown as red, dominates the outer rim of the inner shell and the outer shell of the nebula.

The inner shell has a diameter of 139″. H$\alpha$ and [O III] images show two irregular regions where the surface brightness decreases, known as the eyes of the Owl which are absent in the [N II] image. In [O III] the rim of the inner shell is irregular but rather smooth going outwards, while in [N II] it shows a remarkable interruption in surface bright in the transition region from the inner to the outer shell. The outer shell is practically, with a diameter of 204″for [N II]The surface brightness of the outer shell decreases outwards in H$\alpha$ and [O III] but in [N II] it shows limb brightening.

### *2.0.3. High Resolution Spectroscopy*

We used high-resolution spectroscopic data of the Owl Nebula taken during the nights of 2001 May 22 and 2013 February 17 – 18, employing the Manchester Echelle Spectrometer (MES-SPM) (Meaburn et al. 2003) on the 2.1 m telescope in a $f/7.5$ configuration. Table 1 shows the specification of the CCD and the long slit that were used during the observing runs.

The slit was oriented east-west and exposures were taken at 12 different positions across the nebula, as illustrated in the Figure 3. The exposure times of the spectra were 1800 s. We also took a direct image with 200 s exposure, in which the grating was replaced by a mirror in order to establish the position of the slit at each pointing. Wavelength calibration against the spectrum of a Th/Ar lamp (exposure time of 200 s) was obtained after each science exposure, yielding an accuracy of $\pm$1 km s$^{-1}$ when converted to radial velocity. In this paper all the spectra are in heliocentric

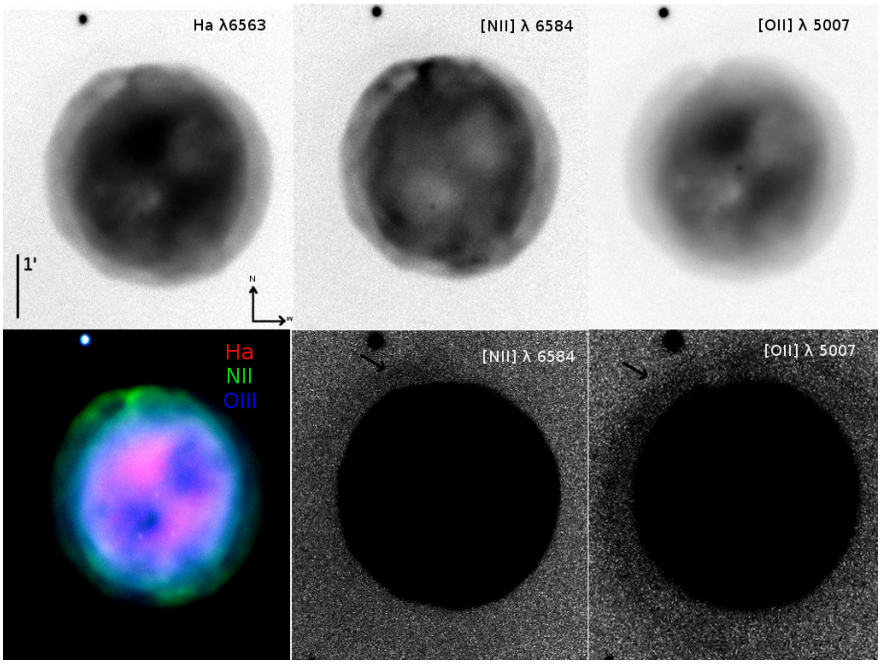


Fig. 2.— Images of NGC 3587 obtained at the OAN-SPM 84 cm telescope, in the light of *TOP:* H$\alpha$ (left panel), [N II] 6584 (center panel) and [O III] 5007 Å (right panel).

| Epoch | no. of frame | CCD | pixels CCD | size pixel $\mu$m | binning | long slit |
|---|---|---|---|---|---|---|
| 2001 | 2 | SiTe3 | 1024×1024 | 24 | 2×2 | 5′.32 |
| 2013 | 10 | Marconi | 2048×2048 | 13.6 | 3×3 | 5′.47 |

velocity ($V_{\rm hel}$). The exact slit position for each pointing were determined astrometrically, using the image plus slit and the positions of nearby stars taken from Digital Sky Survey images and tasks in IRAF. The resultant calibrated spectra are shown in Figure 4. Dust on the spectrograph slit gives rise to instrumental artifacts that can be seen as faint horizontal stripes in the spectra.

In general the position-velocity arrays (PVA), show ellipses characteristic of expanding shells. Long slit spectra of H$\alpha$line emission indicate that NGC 3587 is a closed, nearly spherical shell, showing a smooth outer edge. However, there is limb brightening in [N II]and even the appearance of two separate shell, where one is actually the low ionization outer rim of the inner shell. In slits b, i, j, k, and l the spectra appear "twisted, a behavior also seen in H$\alpha$. These structures are high brightness filaments on the "surface of the inner shell that are captured tangentially in those slits.

The systemic heliocentric velocity calculated in this work was 3 km s$^{-1}$, using the [N II] 6584 PVA, position f (see Figure 4) which cross the main nebula through the center. Using the peak to peak measurement from the integrated PVA through the center of the nebula, the expansion velocity of the inner shell is 35 km s$^{-1}$using [N II] 6584 and 23 km s$^{-1}$ from H$\alpha$. Similarly, the expansion velocity outer shell was 34 km s$^{-1}$ and 18 km s$^{-1}$ measured using [N II] 6584 and H$\alpha$ respectively. These velocities indicate that [N II] is expanding faster than H$\alpha$, and the outer shell is expanding faster than the inner shell. This method to measure the expansion speed differs from the one use by Guerrero et al. (2003) and is meant to correspond to measurements that have been used in statistical analysis on smaller nebulae that can not be resolved as well as the Owl

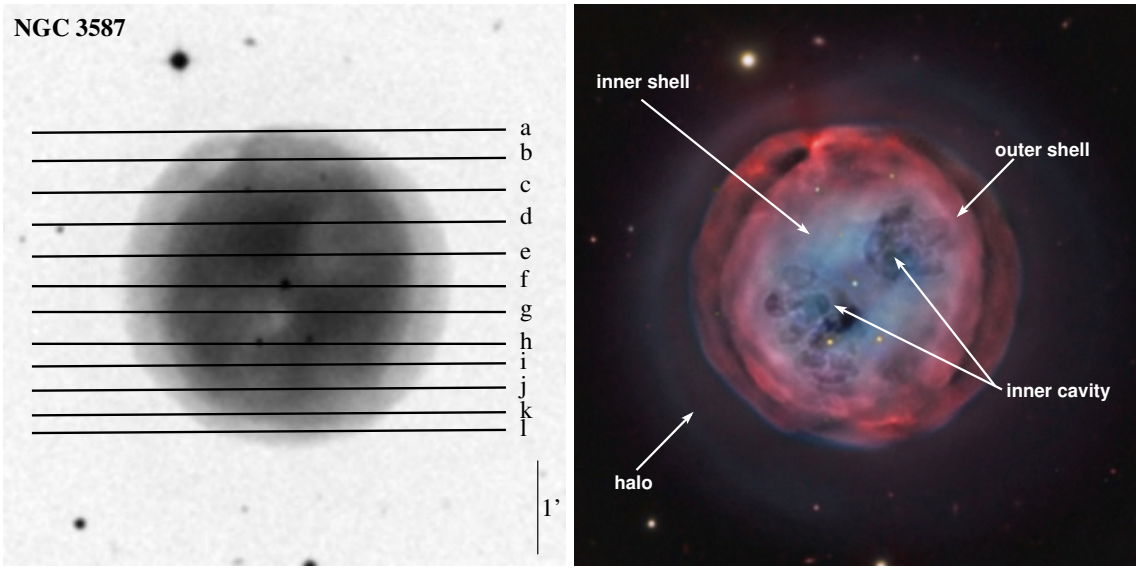


Fig. 3.— Location of each slit position is indicated and labeled on an H$\alpha$ [N II] 6584 image of the Eskimo. North is up, east left. On the right is a NGC 3587 image of combination of the filters Stromgren b, H-beta, O-III, Stromgren y, and H-alpha (image from the Documentary Photo Gallery of Calar Alto Observaotry (CAHA-RECTA-DSA). Vicent Peris (DSA/OAUV), José Luis Lamadrid (DSA/ceFca), Jack Harvey (DSA/SSRO), Steve Mazlin (DSA/SSRO), Juan Fabregat (OAUV), Gilles Bergond (CAHA))

Nebula. Using the method from Guerrero et al. (2003) we obtain similar values as they do.

The inner cavity is best seen in H$\alpha$ and [O III] since this emission comes mainly from the inner volume. The [N II] emission is concentrated in the outer rim of the inner shell and the outer shell. The [N II] rim is irregular and these irregularities correlate with the inner cavity structure to be discussed in more detail below.

## 3. ISOVELOCITY CHANNEL MAPS

In order to assist in the interpretation of the kinematics and the internal structure of the nebula, we constructed iso-velocity channel maps from the parallel and regularly spaced set of PVAs. These are shown in Figure (5) for H$\alpha$and [N II] 6584 together with a direct image (top left), the integrated slits data and the images as reconstructed from the 3-D spectral data cube (top middle). Revelevant features that where found in the maps have been marked in the direct image at the right (top row).

The long-slit echelle spectrocopic data were photometrically calibrated, using the H$\alpha$ and [N II] 6584 images from OAN-SPM (*sec: 2.0.2*) and interpolated to construct position $\times$ position $\times$ velocity maps in H$\alpha$ and [N II] 6584 . We used the techniques described in García-Díaz & Henney (2007) and García-Díaz et al. (2008) to produce the maps. We integrated the surface brightness in a range from $-55$ km s$^{-1}$ to $+65$ km s$^{-1}$ in blocks of 10 km s$^{-1}$ for the reconstructed images at the top of Figure (5).

The individual channels maps have been arranged in such a way to show the corresponding red and blue-shifted velocities one on top of the other, such that the front and back symmetries or asymmetries can be easily identified. The central channel is separate on the right of each sequence.

First of all the well known bipolar structure of the inner cavity is easily identified. Closer inspection does, however, reveal that the south-eastern cavity is actually split in two large regions as marked in the channels for $-15$ km s$^{-1}$ and $+25$ km s$^{-1}$ . Hence we find that there are actually two cavities, with the blue arm pointing more to the east and the red arm pointing more to the south. No such clear split is seen in the north-western cavity.

There also smaller scale splits of the eastern cavity that persist from the channels −35 to −15 km $s^{-1}$ where they merge to a single dark region. These splittings are also very evident in the PVAs. In the morpho-kinematic modeling of the next section, we interpret this split as "fingers" that point roughly towards the observer. They produce the lowest brightness regions near in the direct images near the center of the nebula.

## 4. MORPHO-KINEMATIC MODELING WITH *Shape*

The new data presented in this paper show that the central cavity in NGC 3587 is considerably more complex than the simple bipolar structure proposed earlier. In order to explore whether this complexity has any systematic properties that might produce information about the formation and evolution of the nebula and its central stellar object, we constructed a more detailed morpho-kinematic 3-D model than was available before.

We used the morpho-kinematic polygon based 3-D modeling capabilities of the *Shape* software (Steffen et al., 2011) to model the main features of NGC 3587 concentrating on the inner low emission structure that has been described as bipolar (Guerrero et al., 2003). A dumbbell shaped inner cavity that was proposed by those authors to roughly describe the well known image and the PVAs along the two main axes of the object does not adequately match the substructure that we found in our PVAs and iso-velocity maps. In particular, the eastern dark region with its split sub structure can not be matched, nor can the split structures at even smaller scale in the red and blue-shifted regions. The dumbbell shape can only explain the overall shape of the NW-SSE bipolarity in the direct images.

While quite a number of planetary and proto-planetary nebulae show an overall bipolar structure, the observation of a subdivision into several jet-like features is extremely important to the understanding of the underlying structure-formation mechanism, since it hints towards a complex interaction of a binary central star system. Therefore the exploration of a model for the Owl Nebula that would feature multipolar features for the substructure in the "eyes of the nebula, appears important not only for this particular object.

Finger-like structures become clearly visible in the contrast enhanced image in Figure (3, right). These resemble those of some of the multi-polar planetary nebulae that have been observed and modeled by several authors (e.g. Sánchez-Contreras et al., 2002; Sahai et al., 2005; Sabin et al., 2016; Hsia et al., 2014; Chong et al, 2012; Clark et al., 2012; Velázquez et al., 2011). To our knowledge NGC 3587 is the first to show such a structure as cavities on the inside of a nearly spherical nebula. Potential explanations and the relation to the other types of multi-polar nebulae is discussed in Section 5.

The modeling of the complex cavity inside an otherwise filled H$\alpha$ emission sphere required a somewhat unconventional emission model compared to previous morpho-kinematic models that used *Shape*. We therefore describe this procedure in a bit more detail.

Since we are dealing with a complex cavity, a simple shell model was unsuitable. Rather, the multi-polar cavity has to be "carved out" from a filled sphere. Therefore, the outline of the H$\alpha$ emission was modeled with a slightly prolate ellipsoidal spheroid that was filled with uniform emission. Then the multi-polar cavity structure was build as a polygon volume. However, instead of giving this volume a physical emission property, this volume multiplies any emission inside the volume by some factor smaller than one. It turns out that the volumes are not completely devoid of emission, therefore the multiplier is set to 0.3, constant over the full multipolar structure. This factor is likely to vary considerably over the whole structure, but trying to model this in more detail would have been too complex for technical reasons and would not affect the nature of result that we obtained. In the *Physics Module* of *Shape* the multiplier is generated using a *Scale Species* which is assigned to the cavity structures in the *3-D Module*. All polygon objects which, in the object list of *Shape*, are located below an object with such an object with a *Scale Species* will have this scaling factor applied.

Figure (6) compares a high contrast observed image with the synthetic model image and in Figure (4) the synthetic P-V diagrams are shown (middle) along with the observations. Clearly the multipolar cavity structure is necessary to explain the detailed structure of the image and P-V di-

agram. In particular, note the change from blue to red-shifted cavities in the southern half from the P-V diagrams *g* to *h*, which was impossible to model with a single connected structure such as a dumbbell, even if it was wide ranging from blue to red in terms of Doppler-shift. In the south-west, therefore there must be a group of blue and a group of red-shifted fingers as has already been discussed in Section 3. The polygon model at the bottom right of Figure (6), which was rendered from a vantage point to the west of the line of sight from Earth, clearly shows the two separate S-E groups of fingers as well as the N-W group.

In the N-W group we can identify three different fingers in addition to a larger bubble-like structure that probably was part of the reason for the earlier bipolar interpretation of the cavity structure. In the S-E, the blue group has at least four fingers, whereas we find three in the red-shifted group, plus an uncertain smaller fourth.

## 5. DISCUSSION AND CONCLUSION

We present 12 new high resolution, spectral observations across the Owl Nebula (NGC 3587) and, based on a morpho-kinematic model, we offer a new interpretation of the structure of the internal double cavity that corresponds to the name-giving "eyes" of the nebula.

The images and P-V diagrams in Figures (2) and (**??**) at first sight do not show any evidence for an inclined elliptical or bipolar overall structure of the nebula. However, we found that using an prolate ellipsoidal shape for the inner shell improves the match between model and observation. The ratio between the length and width of the ellipsoid is about 1.13 with a position angle of about 60 degrees and an inclination of approx. 25 degrees (the plane of the sky is zero inclination[CHECK CONVENTIONS]) with the N-W half pointing closer towards Earth. This is consistent with the value 1.12 from the extent of the inner shell axis radii found by Guerrero et al. (2003). The axis of the ellipsoid is roughly aligned with the two multipolar groups of fingers that are themselves building an approximate overall bipolar structure. However, there seems to be a deviation of about 10-20 degrees, but the uncertainty of the inclination of the ellipsoid is rather high being estimated to about 10-20 degrees through trial and error of different values.

The main subject of this paper is the structure of the inner low-brightness cavity and its origin. Guerrero et al. (2005) concluded that we are seeing a bipolar dumbbell shaped cavity. More recent images and our extended coverage with spatially resolved spectral observations leads us to conclude that the structure of the cavity is actually more complex and exhibits multipolar finger-like features. The main surprise is that in the N-W there is not only one group of fingers, but two. The first is roughly align with those in the S-E quadrant, possibly building an overall bipolar structure. However, the second group is almost perpendicular to the axis of the other two, pointing toward Earth. The structure slightly resembles the off-axis structures seen in the proto-planetary nebula CRL 2688 (the "Egg Nebula") in *Hubble Space Telescope* infrared images (Sahai et al., 1998).

In the south-eastern (S-E) lobe we identify three individual "fingers", while the north-western (N-W) lobe has a total of seven, with three on the blue and four on the red-shifted side. From the model it is not immediately clear whether the groups of three fingers come as opposite pairs, which would imply that the origin is probably an episodic bipolar outflow that changed direction for each burst that produced the structures. The length of the fingers is similar, such that they were probably produced in a relatively short time (compared to the age of the complete nebula), putting strong constraints on any model that would generate them as separate ejection events.

The outer [NII] emission shell has an imprint of the fingers although they themselves do not appear to reach out that far. This becomes evident when we compare the P-V diagrams for H$\alpha$ and [NII] in Figure (4). In most directions where there is a finger in the H$\alpha$, the bright [NII] shell shows reduced brightness. Our interpretation of this observation is that the ionizing radiation from the central star can escape further through the fingers and reduces the [NII] emission in the shell since the high ionization states can reach further out along these directions.

It is important to note that there is no evidence of significant edge-brightening of the fingers. Edge-brightening would point towards them being the result of expanding shocks that swept up the gas, which is what would be expected for a wind or

jet being the cause. At this stage we find no evidence for the velocity field to deviate significantly from a homologous expansion, which shows that the inner H$\alpha$ region that contains the cavities is not the region of freely expanding wind. The fast wind from the central star has therefore already ceased or does not extend significantly into the nebula. Therefore, as already proposed by Guerrero et al. (2003), the inner region might be refilling the volume and compressed swept-up gas could be smeared out.

Models that describe multipolar structures in (proto-) planetary nebulae mainly go along two lines. First, episodic collimated outflows from a binary or multiple central star system (e.g. Velázquez et al., 2010) and the expansion of an isotropic fast wind through a dense inhomogeneous circumstellar post-asymptotic giant branch (AGB) wind (Steffen et al., 2013). However it is not clear whether any of these models can apply here. Specific numerical hydrodynamic simulations will be needed to test whether these model can be applied to this case of cavities in the central region of a planetary nebula. A particular problem for those models as applied to the Owl Nebula is that they occur in the pre-planetary or early planetary nebula stage, whereas here the multipolar driving mechanism acts on a more evolved nebula and has not reached its edge.

In conclusion, we have established the multipolar character of the inner low brightness region of the Owl Nebula and have found a new region of cavities that extends roughly perpendicular to the main axis pointing towards the observer. In contrast to other known multipolar planetary nebulae, in NGC 3587 must have formed at a late stage of the nebular evolution.

We thank the daytime and night support staff at the OAN-SPM for facilitating and helping obtain our observations, particularly Gustavo Melgoza, Felipe Montalvo, Salvador Monroy and Francisco Guillen, who were the telescope operators during our observing runs. W.S. acknowledges support from UNAM grants DGAPA PAPIIT 101014 and 104017.

## REFERENCES

Balick B., Alexander J., Hajian A. R., Terzian Y., Perinotto M., & Patriarchi P. 1998, ApJ, 116, 360

Balick, B., Preston, H. L., Icke, V. 1987a, AJ, 94, 1641B

Balick B., Owen R., Bignell C. R., Hjellming R. M. 1987b, AJ, 94, 948

Balick B. 1987c, AJ, 94, 671

Ciardullo, R., Bond, H. E., Sipior, M. S., Fullton, L. K., Zhang, C.-Y., Schaefer, K. G. 1999, AJ, 118, 488

Clark, D. M., García-Díaz, M. T., López, J. A., Steffen, W. G., & Richer, M. G. 2010, ApJ, 722, 1260

Danehkar, A., Frew, D. J.; De Marco, O., & Parker, Q. A. 2011, arXiv1109.2181D

Frew, D. J. 2008, Ph.D. Thesis, Department of Physics, Macquire University, NSW, 2109, Australia

García-Díaz, M. T., Clark, D. M., López, J. A., Steffen, W., & Richer, M. G. 2009, ApJ, 699, 1633

García-Díaz, Ma. T., & Henney, W. J. 2007, AJ, 133, 952G

Gieseking, F., Becker, I., & Solf, J. 1985, ApJ, 295L, 17G

Guerrero, M. A., Chu, Y.-H., Gruendl, R. A., & Meixner, M. 2005, A&A, 430L, 69

Heap, S. R. 1977, ApJ, 215, 864

Kastner et al. 2012, arXiv:1204.6055

Kudritzki, R. P., Mendez, R. H., Puls, J., McCarthy, J. K. 1997, IAUS, 180, 64

López, J. A., Richer, M. G., García-Díaz, M. T., Clark, D. M., Meaburn, J., Riesgo, H., Steffen, W., & Lloyd, M. 2012, RevMexAA, 48, 3

López, J. A., García-Díaz, M. T., Steffen, W., Riesgo, H. & Richer, M. G. 2012a, ApJ, 750, 131

Meaburn, J., López, J. A., Gutiérrez, L., Quiróz, F., Murillo, J. M. & Valdéz, J. 2003, RMxAA, 39, 185M

Méndez, R. H., Urbaneja, M.A., Kudritzki, R. P. & Prinja, R. K. 2011, IAUS 283, submitted.

Natta, A., Pottasch, S. R., & Preite-Martinez, A., 1980, A&A, 84, 284

O'Dell, C. R., Balick, B., Hajian, A. R., Henney, W. J. & Burkert, A. 2002, AJ123, 3329

O'Dell, C. R., Weiner, L. D., & Chu, Y. H. 1990, ApJ, 362, 226

O'Dell, C. R., & Ball, M. E. 1985, ApJ, 289, 526

Pauldrach, A. W. A., Hoffmann, T. L., & Mendez, R. H. 2004, A&A, 419, 1111

Phillips, J. P., & Cuesta, L. 1999, AJ, 118, 2929

Pottasch, S. R., Bernard-Salas, J., & Roelling T. L. 2008, A&A, 481, 393

Reed, D. S., Balick, B., Hajian, A. R., Klayton, T. L., Giovanardi, S., Casertano, S., Panagia, N., &Terzian, Y. 1999, AJ, 118, 2430

Sánchez-Contreras, C., Sahai, R., Gil de Paz, A., 2002, ApJ, 578, 269289

Sahai, R., Sánchez-Contreras, C., Morris, M., 2005, ApJ, 620, 948-960

Sahai, R., Hines, D.C., Kastner, J.H., Weintraub, D.A., Trauger, J.T., Rieke, M.J., Thompson, R.I., Schneider, G., 1998, ApJ, 492, L163-L167

Stanghellini, L. & Shaw, R. A. 2008, ApJ, 689, 194

Steffen, W., Koning, N., Wenger, S., Morisset, C., & Magnor, M. 2010, IEEE, Transactions on Visualization and Computer Graphics, 17, No. 4, 454

Steffen, W., Espíndola, M., Martínez, S., & Koning, N. 2009, RMAA, 45, 143

Steffen, W. & López, J. A. 2006, RMxAA, 42, 99

Steffen, W., Koning, N., Esquivel, A., García-Segura, G., García-Díaz, Ma.T., López, J.A., 2013, MNRAS, 436, 470-478

Tinkler, C. M., Lamers, H.J.G.L.M. 2002, A&A, 384, 987

Velzquez, R., Steffen, W., Raga, A.C., Haro-Corzo, S.A.R., Esquivel, A. Cant, J., Riera, A., 2010,ApJ, 734, 57 (5pp)

Weedman, D. W. 1968, ApJ, 153, 49

Zhang, Y., Fang, X., Chau, W., Hsia, C.-H., Liu, X.-W., Kwon, S., & Koning, N. 2012, arXiv:1205.3470

This 2-column preprint was prepared with the AAS LaTeX macros v5.2.

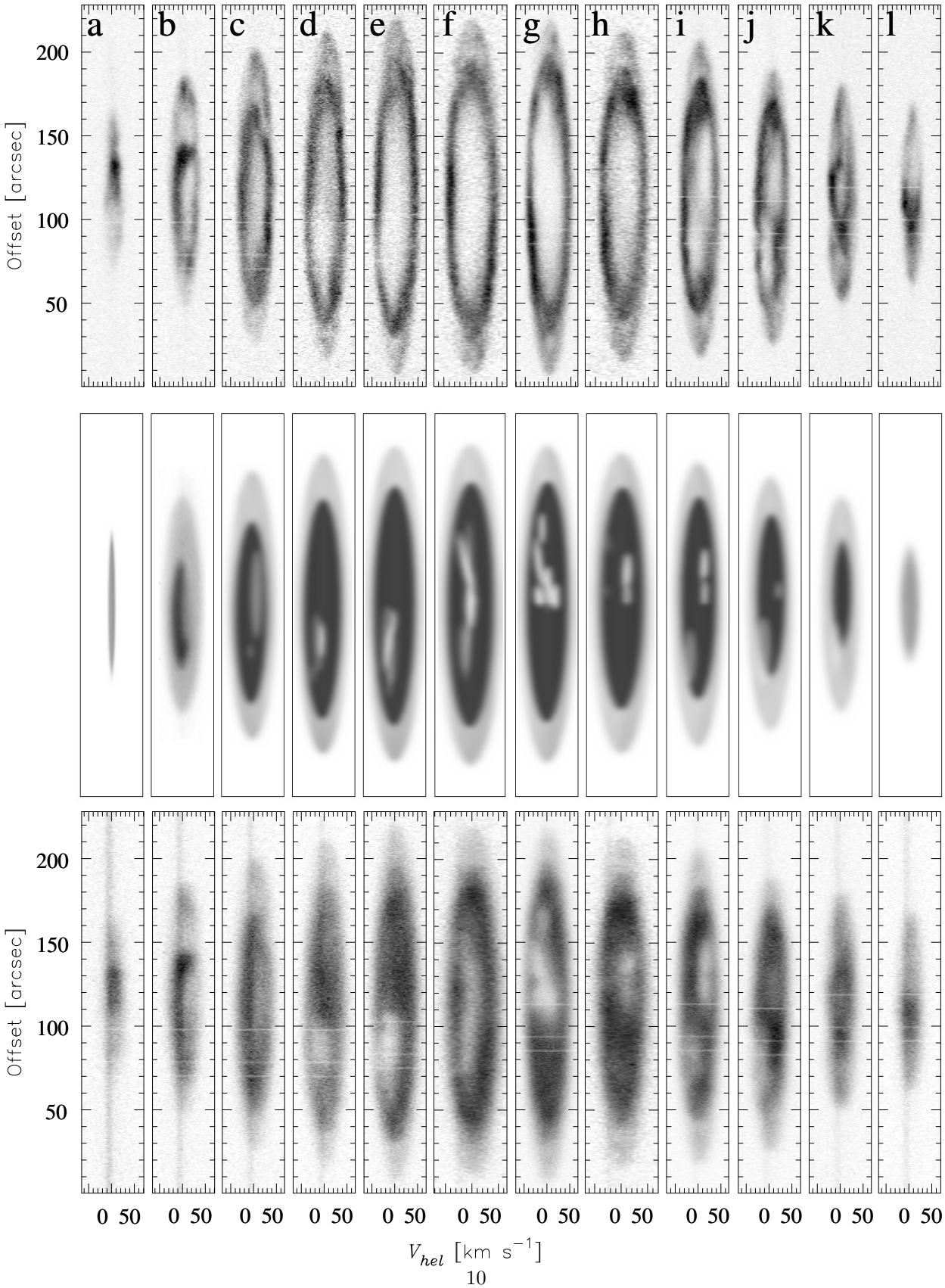


Fig. 4.— Mosaic of bi-dimensional $P$–$V$ arrays labeled according to slit position. For each slit position we show a couple of $P$–$V$ arrays: the observed [N II] 6584 $P$–$V$ array is on the left panel and the corresponding in H$\alpha$ $P$–$V$ array. The top of the array corresponds to the east and left of the slit.

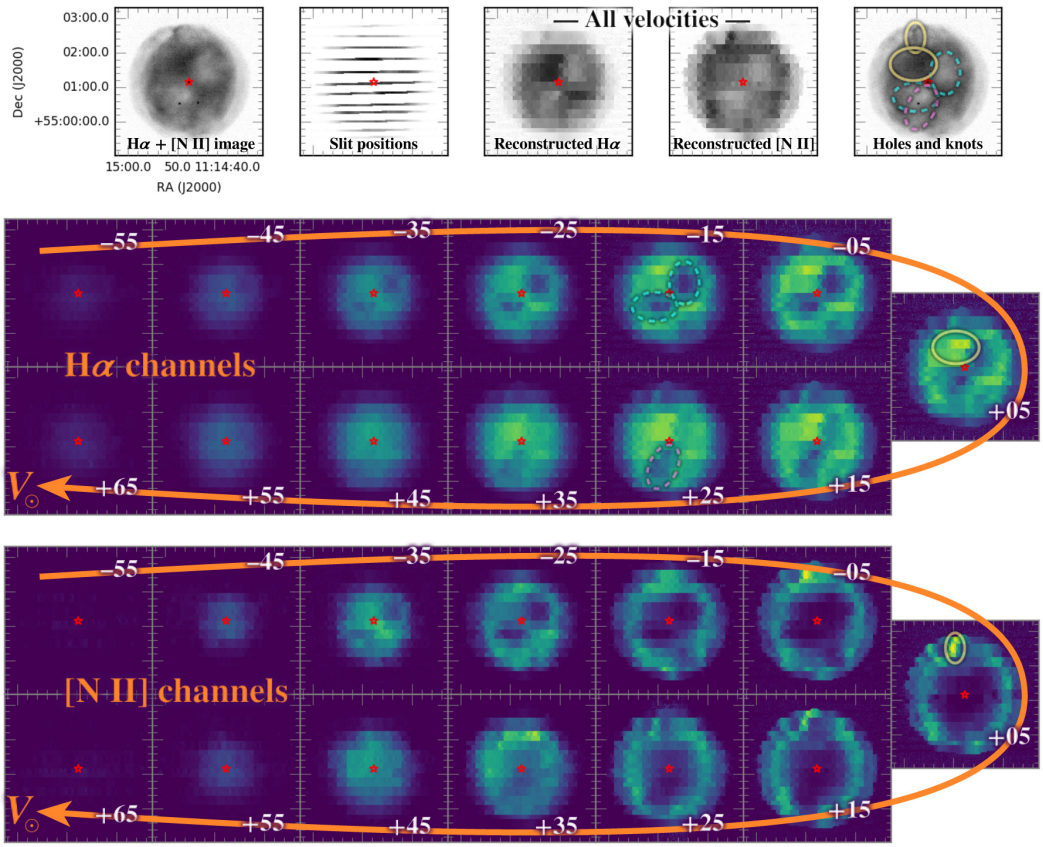


Fig. 5.— H$\alpha$ and [N II] 6584 velocity maps are shown at the top and bottom, respectively.

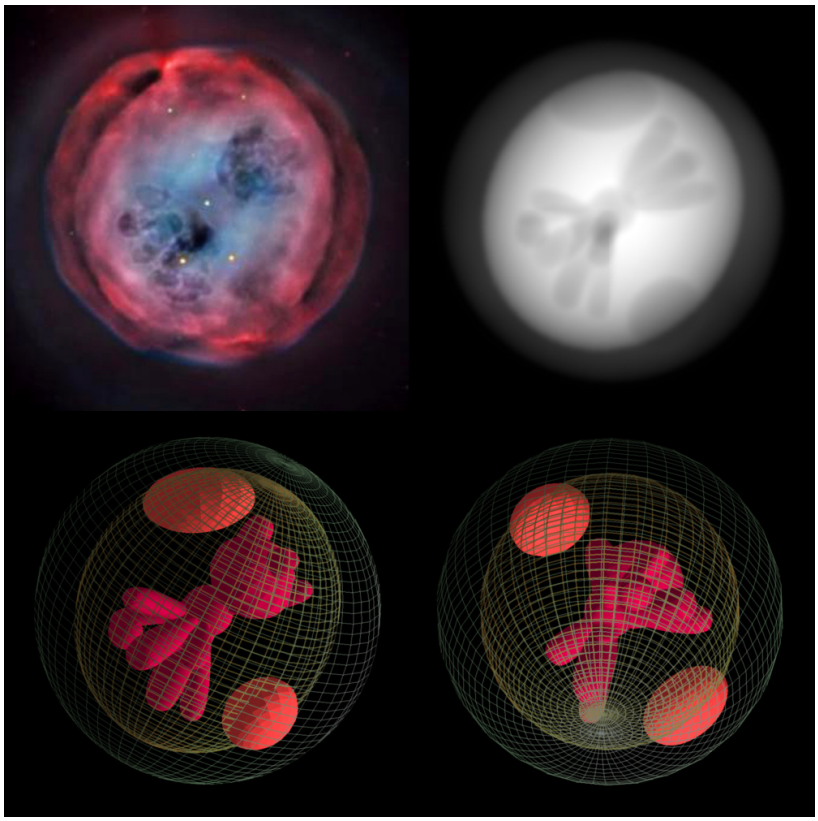

Fig. 6.— A color image of NGC 3587 (top, left) is compared to the grey-scale synthetic $H_\alpha$ image (top, right). Note matching structure of the multipolar inner cavities. At the bottom the corresponding 3-D polygon model structure is shown with two different viewing directions. On the left is the view from Earth that corresponds the images at the top, whereas on the right we have a view from within the plane of the sky with the camera located toward the west of the nebula.